

Review

# Structure Characterisation of Nanoporous Materials using State-of-the-art Single-Crystal X-ray and Neutron Diffraction Techniques

Madeleine Helliwell,<sup>a</sup> John R. Helliwell,<sup>a</sup> Nataša Zabukovec Logar,<sup>b</sup> Gregor Mali,<sup>b</sup> Nataša Novak Tušar<sup>b</sup> and Venc̅eslav Kaučič<sup>b</sup>

<sup>a</sup> School of Chemistry, The University of Manchester, Manchester M13 9PL, UK

<sup>b</sup> National Institute of Chemistry, Hajdrihova 19, 1000 Ljubljana, Slovenia

\* Corresponding author: E-mail: Kaucic@ki.si, Natasa.zabukovec@ki.si, John.helliwell@manchester.ac.uk, Madeleine.helliwell@manchester.ac.uk

Received: 16-04-2008

Dedicated to the memory of Professor Ljubo Golič

## Abstract

A topical review is given of the use of single-crystal characterisation of nanoporous materials, which span applications ranging from catalysis to hydrogen storage including “green chemistry”. This is set in the context of other techniques for characterisation such as NMR, XAS and EELS. The landscape of synchrotron and neutron sources and instrumentation for structure determination is changing both in advances in current provision and proposed upgrades. The complementarity of and synergy between small and large (ie protein) crystallography in our collaboration is also described. A notable step is the ESRF upgrade programme with routine provision for X-ray beams focussed to 50 nm or less.

**Keywords:** Zeolite, nanoporous, X-ray diffraction, synchrotron, neutron diffraction, crystallography, ESRF Upgrade; XAS; NMR; EELS

## 1. Introduction

Microporous solids are an important class of nanomaterials, with pore sizes up to 2 nm, which have many applications as shape selective solid acid catalysts in the oil industry, for the production of fine chemicals and for separations using their molecular sieving capabilities.<sup>1–4</sup> Their great value in modern industrial processes is that they provide a means to cleaner and greener technology, with uses ranging from the synthesis of important chemicals without employing harsh and hazardous chemicals, such as strong acids, or generating green-house gases and other waste products; oxidations can be carried out using mild oxidants such as hydrogen peroxide or O<sub>2</sub> under mild conditions; separations of pollutants, such as radioactive species, ammonia, phosphates, heavy metals and toxic gases from water, soil and air can be carried out using their excellent ion exchange and adsorption properties. Recently, there has also been great interest in the new metal-organic framework structures (MOFs), which have

potential as hydrogen storage materials for applications as alternative energy resources.<sup>5</sup> In order to increase the pore sizes for accessibility to larger reactants, mesoporous silicates and aluminophosphates, with pore sizes from 2–50 nm have been developed. More recently, microporous/mesoporous composite materials have been synthesised, in order to combine the larger pore sizes of the mesoporous materials, with the stable active sites of the microporous component.<sup>6,7</sup>

## 2. Structural Properties of Nanoporous Solids

Microporous inorganic materials are crystalline oxides with a 3D arrangement of TO<sub>4</sub> tetrahedra (T=Si, Al, P, Ga etc.), assembled by the sharing of oxygens, and include zeolites, with aluminosilicate frameworks, and closely related aluminophosphates and gallophosphates (Figure 1a). The size and connectivity of the channels and cavities de-

termine their molecular sieving capability, and importance as shape selective catalysts.<sup>8,9</sup> Substitution of divalent metal atoms leads to modified or improved properties, and the coordination, location and strength of bonding of the divalent transition metal ions in zeolites with different topologies are related to their activity/selectivity in catalytic reactions. An example is nitric oxide (NO) decomposition and the selective catalytic reduction of NO by methane using mordenite or ZSM-5 zeolite.<sup>10</sup> Recently, it has been shown that transition metal ion containing aluminophosphates are active catalysts for a variety of heterogeneously catalysed reactions such as oxidations (MeAPO-5, MeAPO-11 etc., Me=Co, Mn, Fe, Ti, Cr).<sup>11</sup>

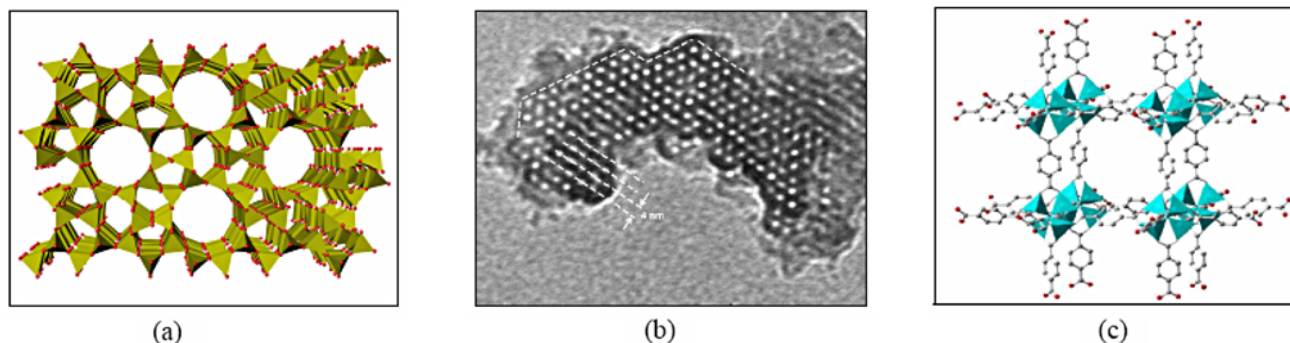


**Figure 1:** (a) Schematic presentation of the zeolitic material showing  $\text{TO}_4$  tetrahedra (T=Si and Al in zeolites, Al and P in aluminophosphates, Ga and P in gallophosphates, etc.), which are connected through oxygen atoms (red spheres) to form a porous structure with channels and cavities up to 2 nm in size, (b) High-resolution transmission electron micrograph (“TEM”) of mesoporous silicate MCM-41 with an hexagonally ordered pore system and pore diameter of 3 nm and (c) a metal-organic framework (“MOF”) structure of MOF-5 built of  $\text{Zn}_4\text{O}(\text{COO})_6$  clusters connected via phenylene rings (ZnO<sub>4</sub> tetrahedra that form the clusters are in turquoise).

Mesoporous inorganic materials are built of  $\text{TO}_4$  units (T = Si, Al, P) that form amorphous structures with ordered pore systems (Figure 1b). The incorporation of transition metals in the mesoporous framework generates catalytic activity of the materials. However, most of the silica- and phosphate-based mesoporous materials have lower catalytic activity and hydrothermal stability than their microporous analogues, which is strongly related to the amorphous nature of the pore walls and severely hinder their practical applications. The recently developed strategy is a two-step preparation of microporous/mesoporous composites, which encompasses the synthesis of nano-sized microporous crystallites that are organised in the mesoporous structure by using large surfactant molecules.<sup>7</sup>

MOFs are inorganic-organic crystalline solids having cavities of uniform size up to 3 nm and an exceptionally large internal surface (Figure 1c). They are constructed by strong covalent bonding of rigid rod-like organic moieties with inflexible inorganic clusters acting as joints. The resulting void spaces are generally moderated by the length and functionalities of the organic units. The majority of experimental work includes the use of transition metal salts as the inorganic source and organic molecules with O or N donor atoms; e.g. the well-known metal-or-

ganic compound denoted MOF-5 is a cubic 3-D porous framework generated by the linkage of  $\text{Zn}_4\text{O}(\text{COO})_6$  clusters via phenylene rings.<sup>5</sup>

### 3. Structure Determination of Nanoporous Solids

#### 3. 1. Microporous Solids

To understand the properties of microporous materials and to design new materials requires their complete characterisation. This includes the determination of the

framework structure, finding the non-framework species, such as template molecules, and finally, and most difficult, the location of the site(s) of the substituted metal atoms and the acidic sites, which confer catalytic activity. It is also important to chart changes, which occur in the production of the active catalysts formed by heating the “as-synthesised” materials; in particular, these include possible oxidation state changes of the incorporated metal atoms and the formation of Brønsted acid sites.

Single-crystal X-ray diffraction gives the most complete answers about the structure properties of ordered crystalline materials. The pre-eminence of single crystal structure analysis has been challenged for this category of crystal due to their generally small volume. Synchrotron radiation chemical crystallography developments have met this challenge.<sup>12</sup> The first steps in the microcrystallography field were by Marjorie Harding using SRS 9.6.<sup>13</sup> Anthony Cheetham, Paul Attfield, Philip Coppens and Jean -Louis Hodeau have also extensively been applying the anomalous dispersion technique.<sup>14–17</sup> Parallel developments in establishing dedicated user facilities have also included Station 9.8 at SRS and the ChemMatCars, a Synchrotron Resource for Chemistry and Materials Science, at APS in particular. We and others have also tak-

en up the challenge of determining low occupancy metal atom substitution.<sup>18</sup> We have also written an extensive summary of the use of anomalous scattering in structural chemistry and biology published in *Crystallography Reviews* in December 2005.<sup>19</sup>

Due to the small size of the crystals and challenge of determining the low-content substituted metal atom sites and their oxidation states, as well as the active acidic sites, a number of other techniques, based on X-ray and neutron diffraction crystal structure determination techniques as well as complementary spectroscopic techniques, have been employed to characterise these materials fully. Two of the leading investigators in the structural characterisation of microporous materials using spectroscopic and/or powder diffraction methods are Sir John Meurig Thomas<sup>20,21</sup> and Lynne McCusker.<sup>22,23</sup>

### 3. 2. Mesoporous Solids

Conventional X-ray diffraction methods fail for structure determination of complex mesoporous materials, nanoparticles or nanospecies encapsulated in mesoporous hosts. At the present moment, a list of complementary characterisation techniques, such as high-resolution transmission electron microscopy (HRTEM) and physical gas adsorption, as well as <sup>29</sup>Si or <sup>27</sup>Al nuclear magnetic resonance spectroscopy (NMR), have to be employed as a support to diffraction and spectroscopic techniques in structural studies of amorphous mesoporous solids and microporous/mesoporous composites.<sup>24–26</sup> Recent developments in microfocus X-ray diffraction also seem to be very promising for structure determination of these materials.<sup>27</sup>

## 4. X-ray Crystallography Characterisation Including Anomalous Scattering for the Metal Based Microporous Catalysts

A successful method of locating and identifying metal atom sites and determining their occupancies in metal-modified microporous solids, is to use the Multiple wavelength X-ray Anomalous Dispersion (MAD) technique; this exploits the large changes in the atomic scattering factor of the particular element in the sample, which take place close to the absorption edges of elements, due to the variation of  $f'$  and  $f''$  with wavelength, where the atomic scattering factor is given by

$$f = f^0 + f' + if'' \quad (1)$$

where  $f^0$  is the scattering factor of the unperturbed atom and  $f'$  and  $f''$  are the real and imaginary components of the anomalous scattering.<sup>14–19</sup> At wavelengths remote

from atomic absorption edges, the anomalous scattering terms are small and vary slowly, but when the wavelength of the X-rays is such that an inner electron can be excited or ejected from the atom, there are large changes in these terms. The position of the absorption edge is element and oxidation state specific. Thus, as we showed with a nickel aluminophosphate sample (NiAPO) using the NSLS<sup>28</sup>, anomalous dispersion experiments can be used to identify and also pinpoint the site(s) of different elements in a compound. In addition, as is widely used in X-ray Absorption Spectroscopy (XAS), a change of valence state alters the edge position slightly, with an increase of valence state of 1, for example, leading to an increase of the absorption edge energy of 2–6eV as the electrons left in the atom are held that much more tightly by the nuclear proton positive charges. This edge shift phenomenon can be utilised in MAD valence contrast experiments, which distinguish between valence states of different specific sites of an element, or to monitor changes in valence state, for example on heating a microporous material to remove the template, and generate the active catalyst.<sup>29</sup> For non-centrosymmetric samples, it is also possible to exploit the large changes in  $f''$  close to the absorption edge, which lead to non-equivalence of Friedel pairs of reflections, and can allow the calculation of anomalous difference maps, to determine the metal atom positions.<sup>18,19</sup> We used the MAD technique to determine and distinguish the site of Co incorporation in the zincophosphate CoZnPO-CZP in a five-wavelength experiment at ELETTRA (Figure 2).<sup>30</sup> Also Cowley, *et al.*, distinguished isoelectronic zinc and gallium cations in the framework of three zinc-gallium phosphates using MAD methods.<sup>31</sup>

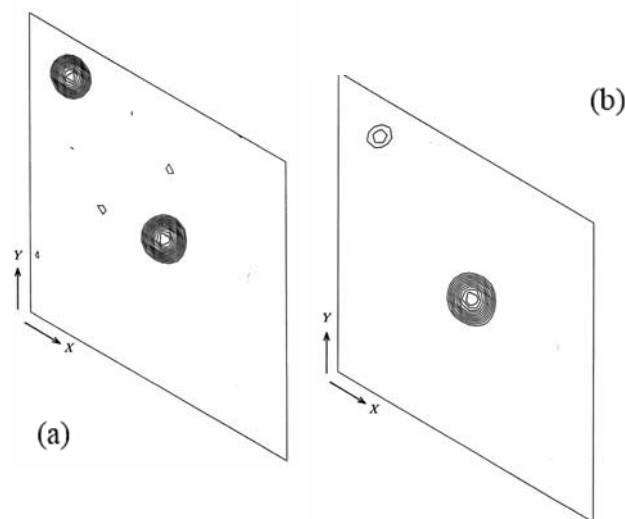


**Figure 2:** Multiwavelength anomalous dispersion (MAD) experiment on the microporous CoZnPO-CZP material. Dispersive difference Fourier maps (a) using the coefficients  $|F_{1.45\text{\AA}} - F_{\text{Zn}^{\text{dip}1}}|$ , show a high concentration of Zn at both crystallographically inequivalent metal sites M1 and M2, (b) using the coefficients  $|F_{1.45\text{\AA}} - F_{\text{Co}^{\text{dip}1}}|$ , show that incorporation of Co had taken place mainly at the M1 site.<sup>30</sup>

## 5. Neutron Crystallography Characterisation Examining Metal Sites in Microporous Catalysts and Sites of Hydrogen Storage Notably in MOFs

The application of neutron diffraction methods to microporous materials complements that of X-ray methods outlined above in a number of ways:

- (i) Hydrogen atoms or alternatively deuterium atoms have scattering powers which are comparable to the heavier atoms in the structure, allowing the determination of their positions in the structure; thus Brønsted acid sites can be seen directly; this is usually not feasible with X-ray diffraction data, because of the low scattering power of hydrogen with X-rays quickly exacerbated by even small amounts of movement. In addition then, MOF samples,<sup>32</sup> which show potential for hydrogen storage, can be investigated using neutron diffraction to see how the hydrogen packs into the cavities.
- (ii) Neutrons provide neighbouring atom contrast based on the fact that different atoms in a structure, of close atomic number, may have quite different neutron scattering lengths, and these are independent of their atomic number and may in addition vary widely for different isotopes of the same element. This latter property has been elegantly harnessed in the determination of the distribution of Ti over the 11 metal atom sites in TiS-1, using isotopic substitution to optimise the element contrast for neutrons.<sup>33</sup> Notably the low atomic number of titanium makes resonant X-ray scattering changes of  $f'$  and  $f''$  with wavelength around the Ti K edge very difficult not least because of the restriction on  $d$  spacings that can be sampled, even at full back-scattering. The neutron approach for Ti is then particularly valuable.
- (iii) Neutrons interact with the nucleus of the atom rather than with the electron charge cloud, so that the atom behaves as a point source, and there is no reduction in scattering factor with angle due to “finite atom size” although obviously affected by mobility or static disorder effects.

Thus there are a number of advantages in harnessing neutrons for the study of microporous materials, particularly for the determination of acidic H atoms, but also for site-specific metal atom identification. Given the variety of metal-atom combinations being synthesised and also that neutrons offer isotopic site-specific contrast that complement the X-ray methods, as well as more definitive hydrogen atom location, neutron diffraction studies, specifically applied to microporous compounds should be more widely used.

With neutrons, in general, the use of deuterated materials is an advantage, first to avoid the high incoherent background seen with  $^1\text{H}$  and secondly because the scattering length for deuterium is larger and positive, in fact equal to carbon. Thus the synthesis of samples using  $\text{D}_2\text{O}$  media can be carried out by methods reported previously.<sup>34</sup> Alternatively exchange of H with D using exposure of samples to  $\text{D}_2\text{O}$  or  $\text{ND}_3$  can be used to obtain fully deuterated samples.<sup>35,36</sup> Calcination of as-synthesised materials leads to the formation of the Brønsted acid sites, which are very important in the catalytic activity of these samples and therefore the determination of these sites is vital in the understanding of reactivity. For the investigation of potential hydrogen storage MOF materials,  $\text{D}_2$  could be incorporated into the cavities for examination by neutron diffraction.

Of course substitution with the heavier deuterium isotope can lead to functional changes known collectively as the “kinetic isotope effect”. The alteration of bond distance for deuterium versus hydrogen is also well documented and in our context very small. A recent assessment of structural changes due to deuteration has been conducted in a survey of the CSD.<sup>37</sup> This recent survey focussed on bond angle changes and concluded that whilst significant differences in structure could be found, the size of the changes was usually small although one instance of a bond angle change upto 20 degrees was found. Overall the “risk” of structural changes due to deuteration was small. In a few cases a different crystal unit cell and space group were obtained; whilst this might be attributable to deuteration it seems more likely that the effect is due to a metastable energy equilibrium of different polymorphs.

In the past, due to the small size of many of the microporous crystals, powder neutron diffraction studies have been most widely used, but if suitable crystals are available, as in the case of X-ray diffraction, the results are more accurate than from powders due to the problems with overlap of reflections that occurs with powder diffraction. One difficulty is the much lower flux of neutron diffraction sources. However a breakthrough in capability has come about with the harnessing of the Laue method, for both protein and smaller molecules at the Institut Laue-Langevin in Grenoble, on new instruments LADI and VIVALDI. An example application is zinc (tris)thiourea sulphate (ZTS), which contains 30 atoms in the asymmetric unit and crystallizes in the orthorhombic space group,  $Pca2_1$ ,  $a = 11.0616$  (9),  $b = 7.7264$  (6),  $c = 15.558$  (1) Å [ $T = 100.0$  (1) K]; the results from a 12 h data collection from ZTS on LADI were comparable with those obtained over 135 h using the monochromatic four-circle diffractometer D9 at the same reactor source with a crystal 13 times larger in volume.<sup>38</sup> Moreover, absorbed atoms have been located using VIVALDI in similar framework structures of crystals of volume  $0.1 \text{ mm}^3$  in just a few hours<sup>39</sup>, and further gains in data-collection efficiency are expected. VIVALDI (a “second generation” successor

device to LADI tailored for small molecules under extreme conditions on a thermal neutron beam) has also been shown to work, with reduced exposure times and smaller crystals, and is tailored to higher resolution work being located on a hotter neutron source.

In some cases it may be possible to determine the crystal structure of a microporous or MOF compound using the single crystal X-ray diffraction technique, but the crystal size may not be sufficient for single crystal neutron Laue diffraction. In these cases, powder diffraction neutron diffraction could be employed allowing the H or D positions to be determined by difference Fourier techniques, and/or dual X-ray and neutron refinement of the two data sets (Figure 3).<sup>40–42</sup>

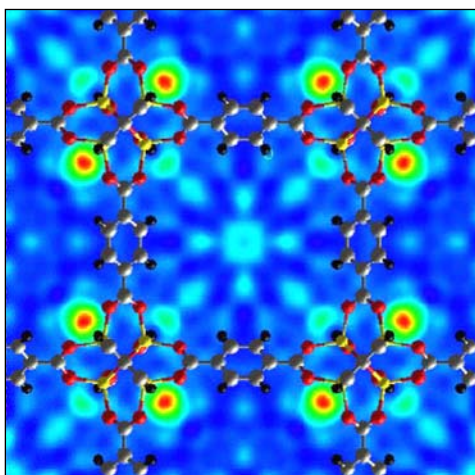


**Figure 3:** The hydrogen adsorption sites in MOF-5 were determined using neutron powder diffraction along with first-principles calculations. The red-green circular objects are the H<sub>2</sub> molecules. The other “fuzzy” peaks in green-white show the noise level of the maps. For clarity, the MOF structure is superimposed (zinc=yellow spheres, oxygen=red spheres, carbon=grey spheres, hydrogen=black spheres). The pressure-dependent study revealed that hydrogen molecules adsorb on the Zn-oxide cluster of the MOF-5 structure even at low pressures. Only at higher pressures does hydrogen also adsorb on the organic linker (terephthalate).<sup>40</sup> (Image credit: Taner Yildirim, National Institute of Standards and Technology)

## 6. Other Techniques:

### X-Ray Absorption Spectroscopy (XAS), Nuclear Magnetic Resonance Spectroscopy (NMR) and Electron Energy Loss Spectroscopy (EELS) for Determination of Low Z Sites and Degree of Order in Metal Based Microporous and Mesoporous catalysts

#### 6.1. X-Ray Absorption Spectroscopy

With the availability of synchrotron radiation sources, X-ray absorption spectroscopy (XAS) techniques

have developed into a widely used tool for structural research of materials in any aggregate state. XAS analytical methods XANES (X-ray Absorption Near-Edge Structure) and EXAFS (Extended X-ray Absorption Fine Structure) provide microscopic structural information of a sample through the analysis of the X-ray absorption spectra of selected atoms. XANES identifies local symmetry and the average oxidation number of the selected atom. EXAFS provides the description of a short-range order for a selected metal centre in terms of the number of neighbours, distances, and thermal and static disorder within the range of those distances. Since XAS is selective towards a particular element and sensitive only towards short-range order around the probed atom, it is one of the most appropriate spectroscopic tools for characterization in the field of catalysis.<sup>43,44</sup> Metal ions, which generate catalytically active sites in metal-modified porous silicates and aluminophosphates, can isomorphously substitute framework elements (Al, P or Si) or can be attached to the aluminophosphate or the silicate framework. Structural characterization of such catalysts by XAS provides the information on the local environment of metal species as well as framework elements.<sup>45,46</sup> With the development of in situ methods, XAS also provides details on the formation process of the catalysts<sup>47</sup> and information on the behaviour of catalytically active sites during the reactions.<sup>48,49</sup> XAS techniques are decisive methods to follow the synthesis pathways and also for the recognition of structural properties that are relevant to the overall optimal performance of a synthesis product as a potential catalyst. Along these lines, the local environment of metals have been studied using XAS in several metal-modified porous aluminophosphates (MeAPO) and metal-modified porous silicates.<sup>4</sup>

#### 6.2. Nuclear Magnetic Resonance Spectroscopy

Solid-state nuclear magnetic resonance (NMR) spectroscopy probes the magnetic environment of nuclei in materials. The technique is very sensitive to changes in coordination environment and can be used as an element specific structure analysing tool.<sup>50</sup> The environments of framework and extra-framework atoms of porous solids can be studied by the NMR spectroscopy of <sup>29</sup>Si, <sup>27</sup>Al, <sup>31</sup>P, <sup>69</sup>Ga or <sup>71</sup>Ga nuclei, or nuclei of charge-compensating ions like <sup>1</sup>H, <sup>7</sup>Li, <sup>23</sup>Na or <sup>133</sup>Cs. Such measurements can readily provide information about the number of inequivalent atomic sites and about the multiplicity of these sites. Recent development of techniques that enable one to probe internuclear distances increased the power of NMR even further. As an example, the structures of two zeolites were recently solved using double-quantum dipolar recoupling NMR spectroscopy, which probed the distance-dependent dipolar interactions between <sup>29</sup>Si nuclei in the framework.<sup>51</sup> The potential of NMR spectroscopy for

structural analysis was enhanced also because of recent progress in the field of ab-initio computational methods, which can now readily predict NMR-observable parameters like chemical shift and quadrupolar coupling parameters.<sup>52</sup> First tests show that combination of NMR spectroscopy and ab-initio calculations is very sensitive to structural variations and can complement X-ray powder diffraction information substantially.

For many years NMR spectroscopy has also been extremely valuable for studying the catalytic properties of porous materials. The fields of application of NMR spectroscopy ranged from the studies of host-guest interactions<sup>53</sup> and the in-situ studies of reactions catalysed by zeolites<sup>54</sup>, to investigations of the structure of Brønsted acid sites<sup>55</sup>. In silicate materials the acid sites are usually generated by partial incorporation of aluminium into the silicate framework. In such materials <sup>29</sup>Si chemical shifts depend sensitively on the number of silicon and aluminium atoms connected with a given SiO<sub>4</sub> tetrahedron. This allows one to quantify the framework Si/Al ratio.<sup>56</sup> The nature and the strength of acid sites can be further investigated by <sup>1</sup>H MAS NMR. In a similar way to acid sites in aluminosilicates, the catalytic centres of microporous and mesoporous aluminophosphates can be obtained by partial substitution of framework aluminium with transition-metal ions. <sup>31</sup>P NMR spectroscopy of aluminophosphates then plays a similar role as <sup>29</sup>Si NMR spectroscopy of aluminosilicates.<sup>57</sup> Recently we have shown that broadline <sup>31</sup>P NMR can be employed for studying Ni(II), Co(II), Fe(II/III) and Mn(III) incorporation, when the extent of substitution, i.e. Me/Al fraction, is above 1% (Figure 4).<sup>58</sup>

<sup>31</sup>P NMR spectroscopy is complementary to XAS techniques, because it provides information about the amount and the location of the incorporated transition metal.

The traditional power of NMR is certainly in its ability to study materials or motifs that lack long-range order. <sup>29</sup>Si magic-angle-spinning (MAS) NMR spectroscopy in silicates and <sup>27</sup>Al and <sup>31</sup>P MAS NMR spectroscopy in aluminophosphates can establish the extent of molecular framework order and the degree of condensation. For example, linewidths in MAS NMR spectra of mesoporous materials can be an order of magnitude larger than the linewidths of MAS NMR spectra of well-crystalline microporous materials. Signals of nuclei in completely condensed Si(OSi)<sub>4</sub> or P(OAl)<sub>4</sub> units can still be resolved from signals of Si(OSi)<sub>3</sub>(OH) or P(OAl)<sub>3</sub>(OH) units of disordered materials. We have studied the extent of framework order and the degree of condensation in mesoporous aluminophosphates and in aluminosilicate composites (Ti,Al)-Beta/MCM-48<sup>59</sup> and (Ti,Al)-Beta/MCM-41<sup>60</sup>, as well as in mesoporous aluminophosphate thin films<sup>61</sup>.

The complementarity of X-ray diffraction, X-ray absorption and NMR techniques is demonstrated in many recent papers of new microporous and mesoporous materials.<sup>62–69</sup> Notably NMR is sensitive to low Z elements, which are out of range of MAD or XAS sensitive elements.

### 6. 3. Electron Energy Loss Spectroscopy

In 2007 Kimoto et al. demonstrated a combination of scanning transmission electron microscopy (STEM)

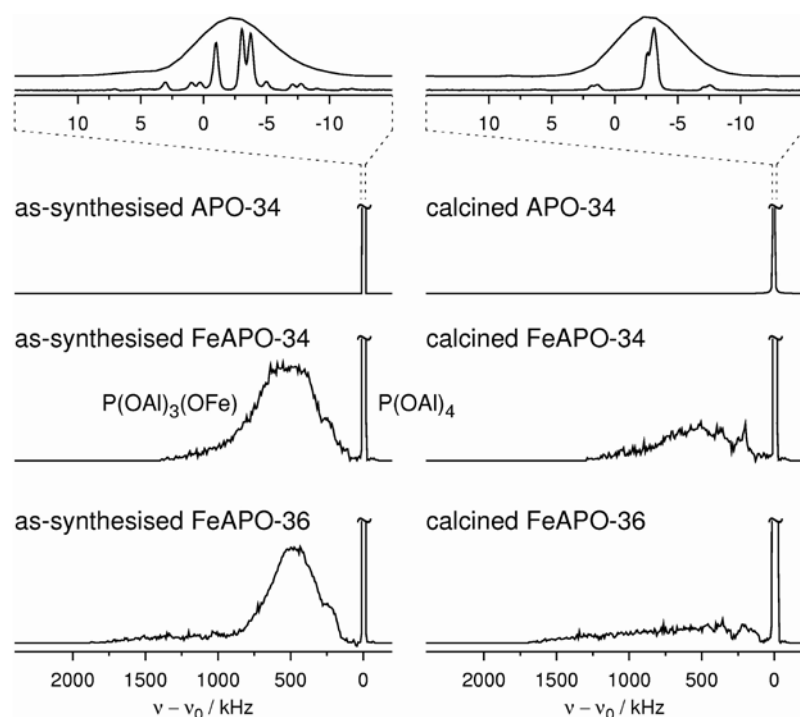


**Figure 4:** Broad-line <sup>31</sup>P NMR can provide direct evidence of the incorporation of iron into the aluminium framework sites of aluminophosphate molecular sieves. Quantitative analysis of NMR spectra can yield information about the distribution and the amount of the incorporated metals. In both FeAPO-34 and FeAPO-36 microporous materials, substantial leaching of iron from the aluminophosphate framework was detected upon calcination.

and electron energy-loss spectroscopy (EELS) in atomic-column imaging of a crystal specimen using localized inelastic scattering and a stabilized scanning transmission electron microscope.<sup>70</sup> In particular, they visualized, as two-dimensional images, the atomic columns of La, Mn and O in the layered manganite  $\text{La}_{1.2}\text{Sr}_{1.8}\text{Mn}_2\text{O}_7$ . A small electron probe, whose diameter was comparable to the interatomic distance in crystals, was scanned over the specimen allowing 10 nm spatial resolution i.e. approximately 4 unit cells spatial sensitivity with the signal from specific elemental atoms revealed. Thus this promises a site occupancy determination over tiny repeat lengths.

If we compare our resonant X-ray scattering “MAD” crystallography approach to determine metal atom site occupancies several points of interest emerge:

- (i) EELS is sensitive to low atomic number elements. Kimoto et al. refer even to oxygen atoms, i.e. well outside of the X-ray crystallography range.<sup>70</sup>
- (ii) Developments at the ESRF with the proposed upgrade<sup>72</sup> will allow X-ray beams down to a size of 50 nm, even 10 nm. Since these will as usual be tuneable to appropriate absorption edges of metal atoms then small length scales akin to EELS can be examined. Like EELS, a column of sample will be sampled, e.g. that might be a lot more unit cells than the spatial width of cca. 4 unit cells.
- (iii) X-rays are not subject to the charging or multiple scattering that arises when using electrons; this may prove to be an important advantage for the ESRF Upgrade applications envisaged here.
- (iv) Kimoto et al. also refer to the presence of an amorphous layer on the sample when preparing the sample for STEM,<sup>70</sup> and which does not apply to the samples studied with X-rays.

Overall, there are significant complementarities as well as independent observation possibilities for the very fine spatial resolution determination of site occupancy parameters with the two approaches. Opportunities would thus allow improved accuracy values and on an incredibly small length scale of 10 nm spatial width. Both techniques remain limited to sampling a column of crystal sample.

Colliex has given an overview News and Views of the Kimoto et al. study and who concluded thus:<sup>71</sup>

“But what is all of this good for? Why is it so important to know the elemental distribution of the atoms in a solid with such a degree of refinement? The choice of specimens by researchers including Kimoto et al. provides a clue. Unusual electronic features, such as the presence of two-dimensional superconducting layers, emerge across or near almost atomically flat interfaces within such complex oxides. Determining as best we can the nature of the atoms concerned and their bonds might help us to discern the patterns underlying such features. Preliminary results are still rather noisy, but the tremendous experimental developments of STEM machines fully targeted to this task will ensure that the ADF–EELS technique

has a bright future in this fast-expanding field of materials science.”

Indeed we would observe that resonant scattering X-ray “MAD” crystallography has also found important applications in pin pointing anomalous scatterers in superconductors (for a review see section 3 of Cianci et al.<sup>19</sup>). Clearly to combine the small spatial width of an X-ray nano-probing tunable ESRF beam with thin specimens, referred to by Colliex, is a big opportunity and of course the biggest challenge for our X-rays approach. Again the ESRF upgrade will come to our aid by giving yet further intensities, reported to be about 4-times higher than the current ESRF levels, through longer straight sections and higher ESRF beam currents.<sup>72</sup>

## 7. Complementarity of Large and Small Molecule Crystallography: the Memories

The occasion when our two research groups came together was an Erice Summer School entitled “Synchrotron Radiation in Crystallography”; John R. Helliwell (JRH) was a lecturer and Slavko Kaučič (SK) was a participant. It was immediately obvious to SK that the instrumentation and methods developments of synchrotron radiation to protein, i.e. large molecule crystallography described by JRH were applicable to SK’s microporous structural and synthetic research. Notably the use of intense synchrotron radiation X-ray beams to study small crystals and the tuneability of synchrotron radiation would allow immediate application to weakly substituted but catalytically important metal aluminophosphates. These two aspects have been the “bread and butter” of our collaboration these last twenty years. Ljubo Golic took a personal and academic interest in these developments, which stimulated us further. Later, after this initial stimulus, the white beam SR Laue crystallography theory, methods of analysis and software migrated from Daresbury SRS to the Institut Laue Langevin neutron research reactor facility. This opened up much more efficient use of the emitted polychromatic neutron beams in neutron protein crystallography, i.e. raising the molecular weight of proteins that can be studied to elucidate their protonation states as well as reducing the crystal sample volume required with the LADI instrument (now LADI III).<sup>73</sup> In chemical crystallography a dedicated LAUE Diffractometer was established by Dr. Garry McIntyre, Dr M Lehman and Dr C Wilkinson and colleagues, named VIVALDI (LADI II in effect).<sup>74</sup> Thus it was intensely satisfying, in our most recent joint research adventure that we were able to use VIVALDI in a study of zinc gallophosphate sample (ZnULM-5). This neutron study complements an 11 wavelength SRS 9.8 study involving eleven data sets recorded at high resolution at X-ray wavelengths

around the Zn and Ga K absorption edges. Unfortunately, the small size of the ZnULM-5 sample, the most challenging crystal volume studied at VIVALDI thus far, proves to be too small at present for a high resolution crystallographic analysis; ie the neutron diffraction data do not extend beyond approximately 1.4 Å and that is therefore too coarse for our purposes.<sup>75</sup>

It is worth mentioning some other protein crystallography developments that have occupied JRH's research efforts in Manchester but have not yet at least made the across-the-disciplines migration to chemical crystallography.<sup>76</sup> Firstly crystallisation using microgravity to create a much more quiescent fluid state has led to a variety of protein crystal quality improvements notably lower mosaicity and higher diffraction resolution as well as more iso-dimensional crystal shapes and larger volumes on average.<sup>77</sup> In a special application by researchers led by Prof DeLucas in Alabama, USA crystallised insulin formulations in microgravity, which had a basically constant crystal size distribution. For the microporous materials, which are crystallised at very high temperatures, the relevance of convection-free fluid microgravity conditions is not apparent but clearly the effects and possible benefit are obvious, if a suitable mechanism could be found. Indeed, in nanotechnology applications the desire for finishing crystal growth at a particular size (nanocrystal size for example) is a technological requirement.

Secondly the use of white beam X-ray Laue diffraction to study photostimulated reactions in a protein crystal on a sub-nanosecond scale, notably at ESRF ID09, has potential in the very fastest photostimulated solid-state reactions in chemical crystallography. Currently synchrotron radiation monochromatic approaches, beautifully pioneered by Coppens and co-workers<sup>78</sup> and latterly by

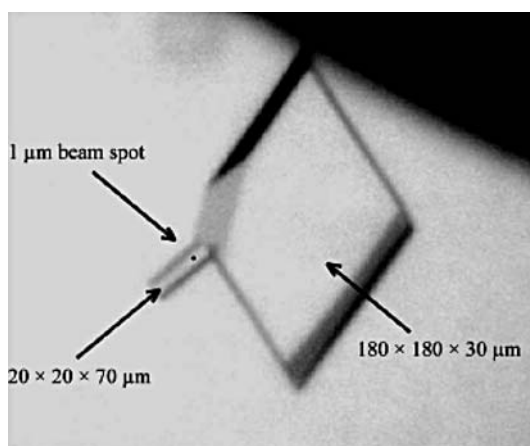


**Figure 5:** ESRF microfocus beam experiment; for the first time, a protein one-micron-beam-crystallography study has been performed ie with a focused synchrotron-radiation beam of 1 μm using a goniometer with a sub-micrometre sphere of confusion. Thus the crystal structure of xylanase II has been determined with a flux density of about  $3 \times 10^{10}$  photons  $s^{-1} \mu m^{-2}$  at the sample.<sup>27</sup> (reproduced with permission from ref. 27)

Raithby and co-workers<sup>79</sup> now have time-resolutions down to the microsecond regime in chemical crystallography.

The future trends in X-ray diffraction and complementary methods are nicely presented in the proposed ESRF Upgrades. They are expected to have an impact across all areas of science and synchrotron radiation based techniques, especially with the provision of routine nano-sized X-ray beams (Figure 5). The proposals developing X-ray diffraction techniques include various nano-diffraction beamlines, a new multi-station beamline to provide a Massively Automated Sample Screening Integrated Facility to screen protein crystals (particularly important for micron-sized samples) for distribution to a renewed suite of macromolecular crystallography stations, and there are ideas to develop coherent diffraction imaging to study individual objects, both from life sciences and the physical sciences. Besides diffraction, but also relevant to the study of nano-scale materials such as those described in this paper, nano-focus EXAFS (with *in situ* extreme T, P environments) and 100 ps time-resolved XAS are planned, amongst others.

## 8. Conclusions

This review has surveyed the contemporary scene for analysing important classes of nanomaterials by diffraction techniques. Complementary techniques of NMR, XAS and EELS to the use of diffraction have also been described. The landscape of synchrotron and neutron facilities is undergoing rapid change and/or dramatic proposed capability changes. These developments should allow important new avenues for structure elucidation. A particular highlight would be sub-micron indeed 10 s of nm sized X-ray beams that would be tunable and allow step scanning of samples for elemental diffraction analysis on the nanoscale.

## 9. References

1. F. Schüth, W. Schmidt, *Adv. Mater.* **2002**, *14*, 629–638.
2. F. Schüth, K. Sing and J. Weitkamp (Eds.), “Handbook of Porous Solids”, Vol. I–V, Wiley-VCH, Weinheim, **2002** and references therein.
3. G. Ferey, *Chem. Mater.* **2001**, *13*, 3084–3098.
4. N. Z. Logar and V. Kaučič *Acta Chim Slov.* **2006**, *53*, 117–135.
5. N. L. Rosi, J. Eckert, M. Eddaoudi, D. T. Vodak, J. Kim, M. O’Keeffe and O. M. Yaghi, *Science* **2003**, *300*, 1127–1132.
6. C. T. Kresge, M. E. Leonowicz, W. J. Roth, J. C. Vartuli and J. S. Beck, *Nature* **1992**, *359*, 710–712.
7. P. Prokesova, S. Mintova, J. Cejka and T. Bein, *Micropor. Mesopor. Mater.* **2003**, *64*, 165–174.
8. J. Cejka and B. Wichterlova, *Catal. Rev.* **2002**, *44*, 375–421.

9. A. Corma and H. Garcia, *Chem. Rev.* **2002**, *102*, 3837–3892.
10. J. Dedecek, L. Capek and B. Wichterlova, *Appl. Catal. A.* **2006**, *307*, 156–164.
11. J. M. Thomas and R. Raja, *Annu. Rev. Mater. Res.* **2005**, *35*, 315–350.
12. W. Clegg, *J. Chem. Soc., Dalton Trans.*, **2000**, 3223–3232.
13. M. M. Harding, *J. Synchrotron Rad.* **1996**, *3*, 250–259.
14. A. K. Cheetham, A. K. and A. P. Wilkinson, *Angew. Chem. Int. Ed. Engl.* **1992**, *31*, 1557–1570.
15. P. Attfield, *Nature*, **1990**, *343*, 46–48.
16. C. T. Prewitt, P. Coppens, J. C. Phillips and L. W. Finger, *Science* **1987**, *238*, 312–319.
17. J. L. Hodeau, V.F. Nicolin, S. Bos, H. Renevier, E. Lorenzo and J.F. Berar, *Chem. Rev.* **2001**, *101*, 1843–1868.
18. M. Helliwell, *J. Synchrotron Rad.* **2000**, *7*, 139–147.
19. M. Cianci, J. R. Helliwell, M. Helliwell, V. Kaučič, N. Z. Logar, G. Mali, and N. N. Tušar, *Crystall. Rev.* **2005**, *11*, 245–335.
20. J. M. Thomas and G. Sankar, *J. Synchrotron Rad.* **2001**, *8*, 55–60.
21. J. M. Thomas, R. Raja, G. Sankar and R. G. Bell, *Nature* **1999**, *398*, 227–230.
22. L. B. McCusker, *Acta Cryst.* **1991**, *A47*, 297–313.
23. L. B. McCusker, C. Baerlocher, R. Grosse-Kunstleve, S. Brenner and T. Wessels, *Chimia*, **2001**, *55*, 497–504.
24. L. A. Solovyov, O. V. Belousov, A. N. Shmakov, V. I. Zaikovskii, S. H. Joo, R. Ryoo, E. Haddad, A. Gedeon and S. D. Kirik, *Stud. Surf. Sci. Catal.* **2003**, *146*, 299–302.
25. K. P. de Jong and A. J. Koster, *Chem. Phys. Chem.* **2002**, *3*, 776–780.
26. A. Zurner, J. Kirstein, M. Dobliger, C. Brauchle and T. Bein, *Nature*, **2007**, *450*, 705–709.
27. R. Moukhametdzianov, M. Burghammer, P. C. Edwards, S. Petitdemange, D. Popov, M. Fransen, G. McMullan, G. F. X. Schertler and C. Riekel, *Acta Cryst.* **2008**, *D64*, 158–166.
28. M. Helliwell, J. R. Helliwell, A. Cassetta, J. C. Hanson, A. Kvik, V. Kaučič and C. Frampton, *Acta Cryst.* **1996**, *B52*, 479–486.
29. J. M. Thomas, G. N. Greaves, G. Sankar, P. A. Wright, J. Chen, A. J. Dent and L. Marchese, *Angew. Chem.* **1994**, *33*, 1871–1873.
30. M. Helliwell, J. R. Helliwell, V. Kaučič, N. Z. Logar, L. Barba, E. Busetto and A. Lausi, *Acta Cryst.* **1999**, *B55*, 327–332.
31. A. R. Cowley, R. H. Jones, S. J. Teat and A. M. Chippindale, *Micropor. Mesopor. Mater.* **1992**, *51*, 51–64.
32. N. Rajic, N. Z. Logar, G. Mali, D. Stojakovic and V. Kaučič, *Croat. Chem. Acta* **2006**, *79*, 187–193.
33. P. F. Henry, M. T. Weller and C. C. Wilson, *J. Phys. Chem. B*, **2001**, *105*, 7452–7458 and references therein.
34. M. T. Weller and N. J. Kenyon, *Stud. Surf. Sci. Catal.* **2004**, *154*, 1349–1355.
35. R. X. Fischer, W. H. Baur, R. D. Shannon, R. D. Staley, L. Abrams, A. J. Vega and J. D. Jorgensen, *Acta Cryst.* **1988**, *B44*, 321–325.
36. F. Gilles, J. L. Blin, C. Mellot-Draznieks, A. K. Cheetham and B. L. Su, *Chem. Phys. Lett.* **2004**, *390*, 236–239.
37. S. Fisher and J. R. Helliwell, *Acta Cryst.* **2008**, *A64*, 359–367.
38. J. M. Cole, G. J. McIntyre, M. S. Lehmann, D. A. A. Myles, C. Wilkinson and J. A. K. Howard, *Acta Cryst.* **2001**, *A57*, 429–434.
39. E. C. Spencer, J. A. K. Howard, G. J. McIntyre, J. L. C. Rowsell and O. M. Yaghi, *Chem. Comm.* **2006**, 278–280.
40. T. Yildirim and M. R. Hartman, *Phys. Rev. Lett.* **2005**, *95*, 215504(4).
41. M. Dinca, A. Dailly, Y. Liu, C. M. Brown, D. A. Neumann and J. R. Long, *J. Am. Chem. Soc.* **2006**, *128*, 16876–16883.
42. Y. Zhao, H. Xu, L. L. Daemen, K. Lokshin, K. T. Tait, W. L. Mao, J. Luo, R. P. Currier and D. D. Hickmott, *PNAS*, **2007**, *104*, 5727–5731.
43. D. C. Koningsberger, B. L. Mojet, G. E. van Dorssen, D. E. Ramaker, *Top. Catal.* **2000**, *10*, 143–155.
44. J. A. van Bokhoven, C. T. Louis, J. Miller, M. Tromp, O. V. Safonova, P. Glatzel, *Angew. Chem. Int. Ed.* **2006**, *45*, 4651–4654.
45. J. A. van Bokhoven, H. Sambe, D. E. Ramaker, D. C. Koningsberger, *J. Phys. Chem. B* **1999**, *103*, 7557–7564.
46. J. Penzien, A. Abraham, J. A. van Bokhoven, A. Jentys, T.E. Muller, C. Sievers, J. A. Lercher, *J. Phys. Chem. B* **2004**, *108*, 4116–4126.
47. D. Grandjean, A. M. Beale, A. V. Petukhov, B. M. Weckhuysen, *J. Am. Chem. Soc.* **2005**, *127*, 14454–14465.
48. J. A. van Bokhoven, A. M. J. van der Eerden and R. Prins, *J. Am. Chem. Soc.* **2004**, *126*, 4506–4507.
49. K. Mathisen, D. G. Nicholson, A. M. Beale, M. Sanches-Sanches, G. Sankar, W. Brass and S. Nikitenko, *J. Phys. Chem. C* **2007**, *111*, 3130–3138.
50. J. D. Epping and B. F. Chmelka, *Curr. Opin. Call. Interfauci.*, **2006**, *11*, 81–117.
51. D. H. Brouwer, R. J. Darton, R. E. Morris, M. H. Leitt, *J. Am. Chem. Soc.* **2005**, *127*, 10365–10370.
52. C. J. Pickard and F. Mauri, *Phys. Rev. B* **2001**, *63*, art. 245101.
53. D. F. Shantz and R. F. Lobo, *Topic Catal.* **1999**, *9*, 1–11.
54. M. Hunger, *Micropor. Mesopor. Mater.* **2005**, *82*, 241–255.
55. M. Hunger, *Catal. Rev. Sci. Eng.* **1997**, *39*, 345–393.
56. G. Engelhardt and D. Michel, *High-Resolution Solid-State NMR of Silicates and Zeolites*, John Wiley & Sons, Chichester, UK, **1987**.
57. L. Canesson, Y. Boudeville and A. Tuel, *J. Am. Chem. Soc.* **1997**, *119*, 10754–10762.
58. G. Mali, A. Ristic and V. Kaučič, *J. Phys. Chem. B* **2005**, *109*, 10711–10716.
59. M. Mazaj, N. Z. Logar, G. Mali, N. N. Tušar, I. Arcon, A. Ristic, A. Recnik and V. Kaučič, *Micropor. Mesopor. Mater.* **2007**, *99*, 3–13.
60. M. Mrak, N. N. Tušar, N. Z. Logar, G. Mali, A. Kljajic, I. Arcon, F. Launay, A. Gedeon and V. Kaučič, *Micropor. Mesopor. Mater.* **2006**, *95*, 76–85.
61. M. Mazaj, S. Costacurta, N. Zabukovec Logar, G. Mali, N. Novak Tušar, P. Innocenzi, L. Malfatti, F. Thibault-Starzyk

- H. Amenitsch, V. Kaučič, G.J.A.A. Soler-Illia, *Langmuir*, **2008**, *24*, 6220–6225.
62. N. N. Tušar, G. Mali, I. Arcon, V. Kaučič, A. Ghanbari-Siahkhalil and J. Dweyer, *Micropor. Mesopor. Mater.* **2002**, *55*, 203–216.
63. A. Ristic, N. N. Tušar, G. Vlaic, I. Arcon, F. Thibault-Starzyk, N. Malicki and V. Kaučič, *Micropor. Mesopor. Mater.* **2004**, *76*, 61–69.
64. A. Ristic, N. N. Tušar, I. Arcon, N. Z. Logar, F. Thibault-Starzyk, J. Czyznievska and V. Kaučič, *Chem. Mater.* **2003**, *15*, 3643–3649.
65. N. N. Tušar, N. Z. Logar, I. Arcon, G. Mali, M. Mazaj, A. Ristic, K. Lazar and V. Kaučič, *Micropor. Mesopor. Mater.* **2005**, *87*, 52–58.
66. N. Z. Logar, N. N. Tušar, G. Mali, M. Mazaj, I. Arcon, D. Arcon, A. Recnik, A. Ristic and V. Kaučič, *Micropor. Mesopor. Mater.* **2006**, *96*, 386–395.
67. N. N. Tušar, N. Z. Logar, I. Arcon, F. Thibault-Starzyk, A. Ristic, N. Rajic and V. Kaučič, *Chem. Mater.* **2003**, *15*, 4745–4750.
68. N. N. Tušar, N. Z. Logar, G. Vlaic, I. Arcon, D. Arcon, N. Daneu and V. Kaučič, *Micropor. Mesopor. Mater.* **2005**, *82*, 129–136.
69. N. N. Tušar, A. Ristic, S. Cecowski, I. Arcon, K. Lazar, H. Amenitsch and V. Kaučič, *Micropor. Mesopor. Mater.* **2007**, *104*, 289–295.
70. K. Kimoto, T. Asaka, T. Nagai, M. Saito, Y. Matsui and K. Ishizuka, *Nature* **2007**, *450*, 702–704.
71. C. Colliex, *Nature* **2007**, *450*, 622–623.
72. ESRF: Science and Technology Programme 2008–2017, volumes 1 and 2 (2007).
73. H. U. Ahmed, M. P. Blakeley, M. Cianci, D. W. J. Cruickshank, J. A. Hubbard and J. R. Helliwell, *Acta Cryst.* **2007**, *D63*, 906–922.
74. G. J. McIntyre, L. Melesi, M. Guthrie, C. A. Tulk, J. Xu and J. B. Parise, *J. Phys. Condens. Matter* **2005**, *17*, 8133–8180.
75. J. R. Helliwell, M. Mozaj, S. Fisher, M. Hellwell, V. Kavčič and G. Melntyre, VIVLADI Experimental Report 5-11-323, Institut Laue Langevin, Grenoble, France (2007).
76. M. P. Blakeley, M. Cianci, J. R. Helliwell and P. J. Rizkallah, *Chem. Soc. Rev.* **2004**, 548–557.
77. E. H. Snell and J. R. Helliwell, *Reports on Progress in Physics*, **2005**, *68*, 799–853.
78. M. Gembicky and P. Coppens, *J. Synchrotron Rad.* 2007, **14**, 133–137.
79. P. R. Raithby, *Crystallography Rev.* **2007**, *13*, 121–142.

## Povzetel

Podan je sistematičen pregled karakterizacij monokristalov nanoporoznih materialov, ki se uporabljajo od katalize do shranjevanja vodika v številni tudi »zeleno kemijo«. Pregled je vpet tudi v druge metode karakterizacij kot npr. NMR, XAS in EELS. Spreminjajo se tudi eksperimentalne metode: sinhrotronski in nevtronski viri radiacije kakor tudi instrumentacija za določevanje kristalnih struktur.